Long Codes for Generalized FH-OFDMA Through Unknown Multipath Channels

Shengli Zhou, *Student Member, IEEE*, Georgios B. Giannakis, *Fellow, IEEE*, and Anna Scaglione, *Member, IEEE*

***Abstract*—A generalized frequency-hopping (GFH) orthogonal frequency-division multiple-access (OFDMA) system is developed in this paper as a structured long code direct-sequence code-division multiple-access (DS-CDMA) system in order to bridge frequency-hopped multicarrier transmissions with long code DS-CDMA. Through judicious code design, multiuser interference is eliminated deterministically in the presence of unknown frequency-selective multipath channels. Thanks to frequency-hopping, no single user suffers from consistent fading effects and constellation-irrespective channel identifiability is guaranteed regardless of channel nulls. A host of blind channel estimation algorithms are developed trading off complexity with performance. Two important variants, corresponding to slow- and fast-hopping, are also addressed with the latter offering symbol recovery guarantees. Performance analysis and simulation results illustrate the merits of GFH-OFDMA relative to conventional OFDMA and long code DS-CDMA with pseudorandom noise codes and RAKE reception.**

***Index Terms*—Blind channel estimation, frequency-hopping, multicarrier CDMA, multipath fading channels, spread spectrum systems.**

I. Introduction

INTRODUCTION of the direct-sequence (DS) code-division multiple-access (CDMA) technology to wireless communications has added many desirable features such as robustness to fading, narrow-band interference suppression and dynamic spectrum sharing. To improve the capacity of CDMA which is interference-limited, many practical systems, e.g., IS-95 [4], utilize symbol aperiodic pseudorandom noise (PN) spreading (the code period is much longer than the symbol period) that distributes users' spectrum over the available bandwidth uniformly. In addition, long scrambling codes enable differentiation of neighboring base stations in a cellular setting [4]. Although they are beneficial to improving capacity of CDMA systems, symbol aperiodic (long) spreading codes do not facilitate the usage of existing (and possibly blind) channel estimation and equalization schemes that have been developed for symbol periodic codes (see, e.g., [5] and references therein). Recently, blind channel estimation algorithms have been proposed for long-code DS-CDMA, both for the uplink [6], [15], [19] as well as for the downlink [13], [18]. Some of the existing uplink channel estimators do not guarantee channel identifiability even when multiple receive antennas are used [6], [15]; alternatively, other methods rely on higher than second-order statistics to assure channel identifiability which can only be checked through computer validation [19]. But even when channel state information (CSI) is utilized at the receiver, decoding requires high-complexity time-varying equalization. Furthermore, multiuser interference (MUI) is only suppressed statistically.

A low-complexity *symbol periodic* CDMA scheme, termed Lagrange–Vandermonde (LV) CDMA, was proposed recently by generalizing orthogonal frequency-division multiple-access (OFDMA) transceivers [14]. LV-CDMA eliminates MUI deterministically in the presence of possibly unknown multipath, but suffers (similar to OFDMA) from channel fading. Compared with other choices explored in [14] to ameliorate the effect of channel nulls, frequency-hopping (FH) offers a vital option because it prevents consistent user-specific fading. For multicarrier CDMA, adaptive FH was also advocated by [2], assuming that CSI is available at the transmitter through a reliable feedback control channel. FH-OFDMA was also proposed in [10] and [11] for CATV transmissions. However, [2], [14] and [10], [11] neither explore blind channel estimation (they rely on training sequences or channel measurements), nor they establish FH-OFDMA links with long-code DS-CDMA.

In this paper, we introduce a general long code CDMA matrix-vector model (Section II) and develop a generalized FH-OFDMA system as a structured long code CDMA system (Section III), to bridge long code DS-CDMA with FH multicarrier transmissions. By adopting symbol-aperiodic Vandermonde–Lagrange codes, generalized FH (GFH)-OFDMA achieves MUI elimination by design over unknown multipath fading and brings FH benefits to long code CDMA, such as avoidance of persistent user-dependent performance degradation from severe fading (Section III). Moreover, thanks to the long code design and by exploiting the finite alphabet property of our source, several novel blind channel estimation alternatives are derived taking into account performance and complexity tradeoffs (Section IV). They guarantee channel identifiability for any finite signal constellation regardless of channel nulls. Based only on the MUI-free demodulated data, they enable simple equalization and are directly applicable

Paper approved by L. Wei, the Editor for CDMA Systems of the IEEE Communications Society. Manuscript received November 1, 1999; revised April 16, 2000 and July 30, 2000. This work was supported by the National Science Foundation Wireless Initiative Grant 99-79443 and the ARL under Grant DAAL01-98-Q-0648. This paper was presented in part at the Wireless Communications and Networking Conference (WCNC), Chicago, IL, September 23–28, 2000.

S. Zhou and G. B. Giannakis are with the Department of Electrical and Computer Engineering, University of Minnesota, Minneapolis, MN 55455 USA (e-mail: szhou@ece.umn.edu; georgios@ece.umn.edu).

A. Scaglione was with the Department of Electrical and Computer Engineering, University of Minnesota, Minneapolis, MN 55455 USA. She is now with the Department of Electrical and Computer Engineering, University of New Mexico, Albuquerque, NM 87131 USA (e-mail: annas@eece.unm.edu).

Publisher Item Identifier S 0090-6778(01)03149-X.

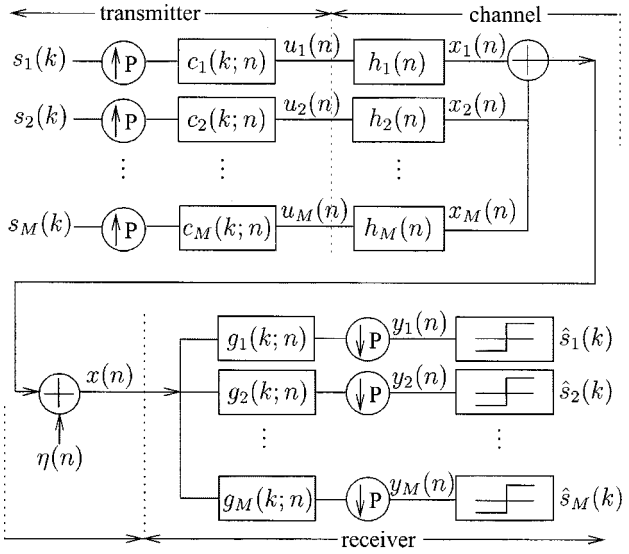

Fig. 1. Discrete-time baseband long code CDMA system.

to single-user OFDM. Symbol recovery can also be assured through fast hopping (Section V). The simulations of Section VI support our conclusions that are summarized in Section VII.

II. System Modeling and Motivation

The block diagram in Fig. 1 describes an equivalent discrete-time baseband model of a CDMA system in the uplink scenario, where signals, codes and channels are represented by samples of their complex envelopes taken at the chip rate. Spreading and despreading are realized by upsamplers and downsamplers, respectively. Related filterbank models were adopted in [16], [14], and [12] for symbol-periodic coded systems. But similar to [19] and [6], our interest is on CDMA systems with long (or symbol aperiodic) codes. Suppose the system can accommodate a maximum of M users. Each of the M users (say the mth user) spreads the information symbols $s_m(k)$ with the upsampler and encodes it using the P-long time varying code $c_m(k;\, n)$, where k signifies symbol-dependence of the chips that are indexed by $n \in [0,\, P-1]$. The mth user's coded chip sequence $u_m(n) = \sum_{k=-\infty}^{\infty} s_m(k) c_m(k;\, n-kP)$ is[1] then pulse shaped to the corresponding continuous time signal $u_m(t) = \sum_{n=-\infty}^{\infty} u_m(n)\varphi(t - nT_c)$, where T_c is the chip period and $\varphi(t)$ is the chip pulse.

The mth user's transmitted signal $u_m(t)$ propagates through a (possibly *unknown*) dispersive channel $h_m(t)$ and is filtered by the receive filter that is matched to $\varphi(t)$ and has spectrum $|\Phi(f)|^2$; we assume here that $|\Phi(f)|^2$ has Nyquist characteristics with frequency support $[-B,\, B]$, where $B \geq 1/(2T_c)$. Let $R_{\varphi\varphi}(t)$ be the convolution of transmit with receive filters, and with $\star$ denoting convolution let $h_m(l) := ((\varphi \star h_m \star \varphi)(t))|_{t=lT_c} = \int_{-\infty}^{\infty} h_m(\tau) R_{\varphi\varphi}(lT_c - \tau)\, d\tau$ be the equivalent discrete time channel impulse response. The mth user's received signal at the chip rate can then be written as

$$x_m(n) = \sum_{k=-\infty}^{\infty} s_m(k) \sum_{l=-\infty}^{\infty} h_m(l) c_m(k;\, n-l-kP). \quad (1)$$

The channel support is assumed to be finite, which is not exact when the bandwidth is strictly limited; however, this approximation is common to wireless environments, where the impulse response support is approximately equal to the maximum path delay plus a few chips. The resulting discrete-time finite-impulse response (FIR) channel filter of order L_m includes the mth user's asynchronism in the form of delay factors as well as transmit–receive filters and multipath propagation. Although our focus will be on the uplink, the downlink scenario is also included in our model; because in the downlink, transmissions from the base station experience a *single common* channel to reach a particular user μ, we have $h_m(l) = h_\mu(l), \forall m \in [1, M]$.

The superposition of all users' signals is received in additive Gaussian noise (AGN), filtered and sampled at the chip rate[2] to obtain: $x(n) := \sum_{m=1}^{M} x_m(n) + \eta(nT_c)$, with η denoting filtered AGN and

$$x_m(n) = \sum_{k=-\infty}^{\infty} s_m(k) \sum_{l=0}^{L} h_m(l) c_m(k;\, n-l-kP) \quad (2)$$

where $L \geq \max(L_1, \ldots, L_M)$ is an upper bound on all FIR channel orders. The sequence $x(n)$ is then correlated with the N_g-long receive-filter $g_m(k;\, n)$ which is equivalent to convolving $x(n)$ with its conjugated and time-reversed version $g_m^*(k;\, N_g - n)$. The resulting output is downsampled by P, and the decision is made based on the estimate

$$\hat{s}_m(k) = \sum_{n=0}^{N_g-1} g_m(k;\, n) x(kP+n). \quad (3)$$

To cast (2) and (3) in vector-matrix form, we define the $P \times 1$ polyphase vectors: $\mathbf{x}(k) := [x(kP),\, x(1+kP),\, \ldots,\, x(P-1+kP)]^T$, $\boldsymbol{\eta}(k) := [\eta(kP),\, \eta(1+kP),\, \ldots,\, \eta(P-1+kP)]^T$, $\mathbf{g}_m(k;\, q) := [g_m(k;\, qP), g_m(k;\, 1+qP),\, \ldots,\, g_m(k;\, P-1+qP)]^T$, the $(L+1) \times 1$ channel vector $\mathbf{h}_m := [h_m(0), h_m(1), \ldots, h_m(L)]^T$, and the $P \times (L+1)$ Toeplitz code matrices

$$\mathbf{C}_m(k;\, q) := \begin{pmatrix} c_m(k;\, qP) & \cdots & c_m(k;\, qP-L) \\ c_m(k;\, qP+1) & \cdots & \vdots \\ \vdots & \ddots & \vdots \\ c_m(k;\, qP+P-1) & \cdots & c_m(k;\, qP+P-L-1) \end{pmatrix}. \quad (4)$$

With $\{\mathbf{x}\}_n$ denoting the nth entry of vector $\mathbf{x}$ and $\{\mathbf{X}\}_{n,l}$ the $(n,\, l)$ entry of matrix $\mathbf{X}$, the received data can be expressed as

$$\begin{aligned} \{\mathbf{x}(k)\}_n &:= x(n+kP) \\ &= \sum_{m=1}^{M} \sum_{k'=-\infty}^{\infty} s_m(k') \sum_{l=0}^{L} h_m(l) \\ &\quad \cdot \{\mathbf{C}_m(k';\, k-k')\}_{n,l} + \{\boldsymbol{\eta}(k)\}_n. \end{aligned} \quad (5)$$

[1]Note that this equation is quite general. In the symbol periodic case, $u_m(n) = \sum_{k=-\infty}^{\infty} s_m(k) c_m(n-kP)$, which unifies many single-user and multiuser modulation schemes, such as OFDM, TDMA/FDMA/CDMA, as detailed in [13].

[2]Note that chip rate sampling is in general suboptimal, but it is common practice (see, e.g., [6], [18], and [19]).

Noting that $\{\mathbf{C}_m(k';\, k-k')\mathbf{h}_m\}_n = \sum_{l=0}^{L}\{\mathbf{C}_m(k';\, k-k')\}_{n,l}h_m(l)$, we obtain from (5)

$$\mathbf{x}(k) = \sum_{m=1}^{M}\sum_{k'=-\infty}^{\infty} s_m(k')\mathbf{C}_m(k';\, k-k')\mathbf{h}_m + \boldsymbol{\eta}(k). \quad (6)$$

Because the P-long codes are convolved with the FIR channels of maximum order L to yield a sequence of length $P+L$, we have from (4) that $\forall k$, $\mathbf{C}_m(k;\, q) \equiv \mathbf{0}$ for $q < 0$ and $q > \lfloor (P+L)/P \rfloor$. Therefore, (6) has only $Q_c := \lfloor (P+L)/P \rfloor$ nonzero terms in the summation over k' and can be rewritten as

$$\mathbf{x}(k) = \sum_{m=1}^{M}\sum_{q=0}^{Q_c} \mathbf{C}_m(k-q;\, q)\mathbf{h}_m s_m(k-q) + \boldsymbol{\eta}(k). \quad (7)$$

Recall that $g_m(k;\, n)$ in (3) has length N_g, define $Q_g := \lfloor N_g/P \rfloor$, and express (3) as

$$\begin{aligned}\hat{s}_m(k) &= \sum_{q=0}^{Q_g}\sum_{n=0}^{P-1} g_m(k;\, qP+n)x(kP+qP+n) \\ &= \sum_{q=0}^{Q_g} \mathbf{g}_m^T(k;\, q)\mathbf{x}(k+q). \end{aligned} \quad (8)$$

Equations (7) and (8) provide a general vector model for symbol-aperiodic DS-CDMA systems that employ long codes as those studied in [6], [18], and [19].

Unlike [6] and [19] that model long PN codes as asymptotically uncorrelated sequences, we in this paper deal with *structured* long *deterministic* codes that (as we shall see subsequently) offer the following:

- deterministic MUI cancellation with a simple linear receiver; and
- blind channel estimation with simple equalization capabilities.

In contrast, note that approaches based on PN codes "randomize" the interference and their success in statistically suppressing it depends on the number of interfering users and the processing gain.

III. GFH-OFDMA with Long Structured Codes

In this section, we seek user codes $\{c_m(k;\, n)\}_{m=1}^{M}$ and receivers $\{g_m(k;\, n)\}_{m=1}^{M}$ that achieve MUI elimination by design. The maximum channel order L may be large in the completely asynchronous case because $L = L_a + L_s$ consists of the maximum asynchronism (L_a chips within a symbol) among all users relative to the user of interest, plus the maximum number of chips L_s caused by the multipath delay-spread (with $\tau_{\max}$ denoting the maximum delay spread, $L_s := \lceil \tau_{\max}/T_c \rceil$; see also [9, p. 797]). In quasi-synchronous (QS) CDMA however, mobile users attempt to synchronize with the base-station's pilot waveform and thus L_a is small [3]; note also that the delay spread in urban environments rarely exceeds 5 μs, while a typical code length in the IS-95 standard is 200 μs (see also [18]); hence, L_s and consequently L can he considered small given our design choice $P \gg L$ that we adopt henceforth. With $P \gg L$, we have $\mathbf{C}_m(k;\, q) = \mathbf{0}$, for $q \neq 0,\, 1$, which allows us to rewrite the kth received data block $\mathbf{x}(k)$ in (7) as

$$\begin{aligned}\mathbf{x}(k) = &\sum_{m=1}^{M} \mathbf{C}_m(k;\, 0)\mathbf{h}_m s_m(k) \\ &+ \sum_{m=1}^{M} \mathbf{C}_m(k-1;\, 1)\mathbf{h}_m s_m(k-1) + \boldsymbol{\eta}(k) \end{aligned} \quad (9)$$

with the second sum in (9) representing the interblock interference (IBI).

Targeting a simple receiver structure for the data in (9), we will concentrate only on a *single block* containing the current symbol $s_m(k)$. Such an IBI-free reception for the user of interest μ is possible, if the receiver $\mathbf{g}_\mu(k)$ satisfies: $\mathbf{g}_\mu^T(k)\mathbf{C}_m(k-1;\, 1) = \mathbf{0}^T$, $\forall\, m \in [1,\, M]$, $m \neq \mu$, which implies that $\mathbf{g}_\mu(k)$ must lie in the intersection of left null spaces $\bigcap_{m\neq\mu}\mathcal{N}(\mathbf{C}_m(k-1;\, 1))$. To characterize the left null space of $\mathbf{C}_m(k-1;\, 1)$, we first note that for the code length $P > L$, the only nonzero entries of $\mathbf{C}_m(k-1;\, 1)$ in (4) appear in the first L rows that form an $L \times L$ full rank (upper triangular) submatrix. Furthermore, $\mathcal{N}(\mathbf{C}_m(k-1;\, 1))$ is spanned by the canonical vectors (one unity entry and all other entries zero) that select the $P-L$ null rows of $\mathbf{C}_m(k-1;\, 1)$. Hence, the only possibility for IBI-free reception is for $\mathbf{g}_\mu^T(k)$ to have its first L entries equal to zero which amounts to discarding the first L chips of the received block. By discarding L chips, as in a standard OFDM system with cyclic prefix [1], IBI is removed and a low-complexity receiver becomes available. Having selected the block length $P \gg L$, the power penalty incurred when discarding L chips becomes negligible[3] (see also [18]).

A. MUI Eliminating Transceivers

Since we have only $P-L$ chips to convey information from M users, a necessary condition to guarantee MUI-free symbol recovery is $P-L \geq M$. Usually, the maximum number of users that can be accommodated by the available bandwidth satisfies $M \gg L$. To avoid overexpansion of bandwidth, we adopt the minimum possible P in our system design by selecting $P = M+L$. To achieve MUI elimination, we design our transceivers as follows: For the kth symbol of user m, we assign a complex number $\rho_{m,\,k}$ to construct the spreading code as (see also [14], [17]):

$$\begin{aligned}\mathbf{c}_m^T(k) &:= [c_m(k;\, 0)\cdots c_m(k;\, P-1)] \\ &= A_m[\rho_{m,\,k}^{-P+1}\cdots\rho_{m,\,k}^{-1},\, 1] \end{aligned} \quad (10)$$

where A_m is the mth user's amplitude. We term $\rho_{m,\,k}$ as user m's *signature point* (when $\rho_{m,\,k}$ is on the unit circle, it can be thought of as user m's subcarrier). Different from [14] and [17], we will allow here $\rho_{m,\,k}$ to change periodically from symbol to symbol with period R ($\rho_{m,\,k+iR} = \rho_{m,\,k}$, $\forall i$, $\forall m$), which leads to long but structured deterministic spreading codes with period RP.

[3]The power penalty can be avoided (when nonzero IBI is allowed) with more complex (and perhaps nonlinear) receiver structures processing multiple blocks. However, linear low-complexity equalization has been among the major advantages of multicarrier systems and motivates our GFH-OFDM designs that target simple transceiver structures.

As we argued earlier, prefixing the μth user's $1 \times P$ receive-vector $\mathbf{g}_\mu^T(k) := [0 \cdots 0, \overline{g}_\mu(k; M-1) \cdots \overline{g}_\mu(k; 0)]$ by L leading zeros avoids IBI. The correlation of this vector with the lth delayed version of mth user's code is therefore: $\sum_{n=0}^{M-1} \overline{g}_\mu(k; n)\rho_{m,k}^{-(n+l)} = \rho_{m,k}^{-l}\mathcal{G}_\mu(k; \rho_{m,k})$, where $\mathcal{G}_\mu(k; z) := \sum_{n=0}^{M-1} \overline{g}_\mu(k; n)z^{-n}$. To ensure MUI elimination, $\mathcal{G}_\mu(k; z)$ must satisfy $\mathcal{G}_\mu(k; \rho_{m,k}) = \theta_{\mu,k}\delta(m-\mu), \forall\, m \neq \mu$, where $\theta_{\mu,k}$ is a constant. The μth user's receiver transfer function that eliminates MUI is then constructed by forming $\mathcal{G}_\mu(k; z)$ as the Lagrange interpolating polynomial through the points $\rho_{m,k}$, $m \neq \mu$

$$\mathcal{G}_\mu(k; z) := \sum_{n=0}^{M-1} \overline{g}_\mu(k; n)z^{-n} = \frac{1}{A_\mu} \frac{\prod_{m=1, m\neq\mu}^{M} (1 - \rho_{m,k}z^{-1})}{\prod_{m=1, m\neq\mu}^{M} (1 - \rho_{m,k}\rho_{\mu,k}^{-1})}. \quad (11)$$

Direct substitution from (4), (10), and (11) verifies that $\mathbf{g}_\mu^T(k)\mathbf{C}_m(k) = \mathbf{0}^T, \forall\, m \in [1, M]$, $m \neq \mu$ and $\mathbf{g}_\mu^T(k)\mathbf{C}_\mu(k) = [1, \rho_{\mu,k}^{-1}, \ldots, \rho_{\mu,k}^{-L}]$. Therefore, we have $\mathbf{g}_\mu^T(k)\mathbf{C}_\mu(k)\mathbf{h}_\mu = \sum_{l=0}^{L} h_\mu(l)\rho_{\mu,k}^{-l} := H_\mu(\rho_{\mu,k})$, and the decoder output of user μ is obtained as

$$y_\mu(k) = \mathbf{g}_\mu^T(k)\mathbf{x}(k) = H_\mu(\rho_{\mu,k})s_\mu(k) + \eta_\mu(k) \quad (12)$$

where $\eta_\mu(k) := \mathbf{g}_\mu^T(k)\boldsymbol{\eta}(k)$ is colored AGN. We infer from (12) that MUI is eliminated deterministically. To recover the μth user's symbols from (12), we employ the maximum-likelihood symbol by symbol detector: $\hat{s}_\mu(k) = \arg\min_s |y_\mu(k) - H_\mu(\rho_{\mu,k})s|^2 = \arg\min_s |y_\mu(k)/H_\mu(\rho_{\mu,k}) - s|^2$, which amounts to the simple equalization scheme

$$\hat{s}_\mu(k) = y_\mu(k)/H_\mu(\rho_{\mu,k}) \quad (13)$$

followed by hard decisions, provided that $H_\mu(\rho_{\mu,k}) \neq 0$. Note that transmissions $s_\mu(k)$ could be, e.g., convolutionally coded, in which case the soft Viterbi algorithm can be applied as detailed in [9, Ch. 8]; however, in this paper, we focus on uncoded transmissions and adopt (13) which offers computationally simple maximum-likelihood symbol-by-symbol detection in the frequency domain.

B. Low-Complexity System Designs

Although [14], [17] also relied on symbol-periodic Vandermonde/Lagrange spreading/despreading like those in (10) and (11), our symbol-aperiodic design herein offers additional flexibility. To appreciate it, let us express $\rho_{m,k}$ as the product of two complex numbers: $\rho_{m,k} = \rho_m\xi_k$. Our codes in (10) will then have entries

$$c_m(k; n) = \tilde{c}_m(n)\overline{c}(k; n) := \rho_m^{-P+1+n}\xi_k^{-P+1+n} \quad (14)$$

where $\tilde{c}_m(n) = \rho_m^{-P+1+n}$ is a user-specific symbol periodic code, while $\overline{c}(k; n) = \xi_k^{-P+1+n}$ changes from symbol to symbol, but is common to all users. Recall that in IS-95, the overall spreading code is the product of a short Walsh–Hadamard code with a long PN-sequence that has period 2^{15}. By explicitly utilizing the "IS-95 like" code structure, we can ease our long deterministic code assignment by:

- constructing each user's symbol periodic code $\tilde{c}_m(n)$ from sufficiently separated (e.g., equispaced around the unit circle) signature points;
- changing only $\overline{c}(k; n)$ from symbol to symbol, with a pattern that is predetermined by the base station and is common to all users.

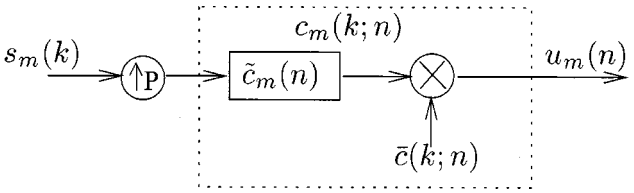

Fig. 2. The mth user's structured long code transmission model.

The spreading procedure is illustrated in Fig. 2 and offers great flexibility in selecting signature points, as we highlight next in several computationally simple designs:

Special Case 1: Here we assign $\rho_m = \exp(j2\pi m/M)$ and $\xi_k = \exp(j\theta_k)$. The overall spreading code vector in (10) will then have entries

$$c_m(k; n) = e^{-j((2\pi/M)m+\theta_k)(P-1-n)}. \quad (15)$$

Substituting $\rho_{m,k}$ in (11) with the $c_m(k; n)$ of (15), we find the receiver filter coefficients $g_m(k; n) = \exp\{j(2\pi m/M + \theta_k)(P-1-n)\}$, $\forall\, n \in [L, P-1]$, which are matched to the transmitted spreading code (15). By setting $\theta_k = 0$, (15) corresponds to a conventional OFDMA transmission.

On the other hand, with varying θ_k we obtain an FH-OFDMA system, which explains why we term our system GFH-OFDMA. When θ_k is a multiple of $2\pi/M$, not only the precoding but also the decoding operation can be implemented by an M-point fast Fourier transform (FFT) (as with conventional OFDMA) followed by a constant permutation matrix, which is determined by θ_k. For example, setting $\theta_k = (k \bmod M)2\pi/M = \overline{k}2\pi/M$, $\overline{k} \in [0, M-1]$, corresponds to the one-step frequency shift hopping pattern of [10], where each user is assigned a frequency that is shifted cyclically over the entire bandwidth. Performing an M-point FFT of the received block yields the vector $\tilde{\mathbf{x}}(k)$ corresponding to the pre-equalized symbols transmitted over frequencies $\{0, 2\pi/M, \ldots, 2\pi(M-1)/M\}$. Let $\mathbf{e}_n$ denote the nth canonical $M \times 1$ Euclidean basis vector, and the $M \times M$ permutation matrix be defined as: $\prod_k := [\mathbf{e}_{\overline{k}+1}, \ldots, \mathbf{e}_M, \mathbf{e}_1, \ldots, \mathbf{e}_{\overline{k}}]^T$. Because the kth symbol of user m is transmitted over the subcarrier $\exp(j2\pi(m + \overline{k})/M)$, multiplying vector $\tilde{\mathbf{x}}(k)$ by $\prod_k$ will deliver the corresponding pre-equalized data (12) to each user. Such an FFT-based decoder followed by the simple equalizer in (13) constitutes our low-complexity receiver. An important extension to the one-step FH could be the Λ-step FH (with Λ an integer $> M/L$) which increases the FH size from $2\pi/M$ to $2\pi\Lambda/M$ (see also [11], where $\Lambda = 4$). Successive symbols in such an Λ-step FH transmission rely on frequencies that are sufficiently separated and are not affected by the same channel null. This leads to independently faded symbols and playing

a role similar to interleaving, it enhances the effect of error control coding.

With spreading codes selected as in (15), the equalizer (13) inverts $H_\mu(e^{-j(2\pi\mu/M+\theta_k)})$. When $\theta_k = 0$, it is impossible (or difficult) to equalize channels with unit circle zeros located at (or close to) angles $2\pi\mu/M$. Through the offset θ_k, our symbol-aperiodic code $c_\mu(k;\, n)$ alleviates such a problem by hopping each user's subcarrier frequency from one symbol to the next.

Special Case 2: Here, we assign $\rho_m = r_m \exp(j2\pi m/M)$ that corresponds to equispaced signature points around co-centric circles of possibly unequal radius. We also choose $\xi_k = r_k \exp(j\theta_k)$, which offers freedom to tune both the code amplitude $r_m r_k$ as well as the phase $2\pi(m/M)+\theta_k$. With flexibility in assigning signature points, GFH-OFDMA gains resilience to Doppler effects or carrier offsets over plain OFDMA as detailed in [12] and [14]. Note that $\rho_m = [1 + 0.1\cos(\pi m/2)]$ $\exp(j2\pi m/M)$ and $\xi_k = 1$ was also proposed in [12] without hopping. Transceivers for this special case will still have low complexity because the corresponding filters can be precomputed for a predetermined hopping pattern and each user can be demodulated using a simple inner-product $\mathbf{g}_m^T(k)\mathbf{x}(k)$. With $r_m = r_0$, $\forall m$, and noting that we are computing the frequency response on a circle with radius $r_{k,e} = r_0 r_k$, complexity can be reduced further by performing an M-point FFT to the received data block weighted by $[1, \ldots, r_{k,e}^{-(M-1)}]^T$ (or by using other chirp $\mathcal{Z}$-transform variants).

Our derivation in this section has shown how FH benefits are brought into general multicarrier CDMA (and particularly OFDMA) systems through structured deterministic symbol-aperiodic long codes. Our simulations will also illustrate that unlike conventional OFDMA, users in GFH-OFDMA will not suffer from severe fading consistently because FH prevents consecutive symbol fading caused by channel nulls. The following proposition summarizes the basic results of this section:

Proposition 1: The GFH-OFDMA transceivers of (10) and (11) constitute a structured long code CDMA system, which bridges long code CDMA with frequency-hopping multicarrier transmissions. Proper design of (10) and (11) allows for IBI removal and deterministic MUI elimination in the presence of frequency-selective multipath.

Novel blind channel estimators become available through hopping user's signature points, as we describe next.

IV. Blind Channel Estimation

Blind channel estimators will be derived in this section by capitalizing on the finite alphabet of the source. The statistics needed to perform channel estimation require data averaging across periods of our long code $c_m(k;\, n)$. Recalling that each $\rho_{m,k}$ is periodic in k with period R, we can write for $r \in [0,\, R-1]$, our symbol index as $k = iR + r$, where i will henceforth index blocks of symbols. Assigning a double argument $(i;\, r)$ to quantities with argument k, we can, e.g., express our GFH-OFDMA received data in (12) as

$$y_m(i;\, r) = H_m(\rho_{m,r}) s_m(i;\, r) + \eta_m(i;\, r) \qquad (16)$$

where $\rho_{m,\,r}$ depends only on r (and not i) because of the code periodicity.

Unlike existing channel estimation methods that are based on the received chip sequences [6], [18], [19], our methods will rely on the MUI-free receiver output (16); and channel estimation will thus be performed separately for each user. For this reason, we concentrate only on the user of interest and drop subscript m (denoting the mth user) for notational brevity. Notwithstanding, an important application of the ensuing algorithms is for single-user multicarrier (e.g., standard OFDM [1]) scenarios.

A. Channel Identifiability

We will start with channel identifiability issues from $y(i;\, r) = H(\rho_r) s(i;\, r)$, where we have not only dropped user indices but also omitted noise since we are concerned with basic feasibility questions first. Considering a general signal constellation with points $\{\zeta_q\}_{q=1}^Q$ on the complex plane, the following must hold: $\prod_{q=1}^Q [s(i;\, r) - \zeta_q] = 0$, since $s(i;\, r)$ is drawn as one of the $\{\zeta_q\}_{q=1}^Q$ constellation points. Expanding the product yields a Qth-order polynomial in $s(i;\, r)$

$$s^Q(i;\, r) + \alpha_1 s^{Q-1}(i;\, r) + \cdots + \alpha_Q = 0 \qquad (17)$$

where $\alpha_1, \ldots, \alpha_Q$ are determined from $\{\zeta_q\}_{q=1}^Q$ and can not all be zero. Let α_J be the *first nonzero coefficient* satisfying $\alpha_j = 0$, $\forall\, j \in [1,\, J-1]$ and $\alpha_J \neq 0$.

Starting from (17), we establish in Appendix I that $H^J(\rho_r)$, the Jth power of $H(\rho_r)$, can be obtained from sufficiently collected noise-free receiver outputs of (16) for $r = 0, \ldots, R-1$.

To express $H^J(\rho_r)$ in terms of $h(n)$, we first define $\boldsymbol{\beta}_J^T := [\beta_0, \ldots, \beta_{JL}] = h(n) \star_J h(n)$ the J-fold convolution of $h(n)$ with itself that we denote as $\star_J$. It then follows that

$$\begin{aligned} H^J(\rho_r) &:= H^J(z)|_{z=\rho_r} \\ &:= (\beta_0 + \cdots + \beta_{JL} z^{-JL})|_{z=\rho_r}. \end{aligned} \qquad (18)$$

To determine the coefficients $\beta_0, \ldots, \beta_{JL}$ uniquely from $H^J(\rho_r)$, we need $JL+1$ distinct such equations that become available when ρ_r takes $JL+1$ distinct values. Therefore, when $R \geq JL+1$ and $\{\rho_r\}_{r=0}^{R-1}$ are distinct, we can find $\beta_0, \ldots, \beta_{JL}$ uniquely, which enables determination of $H^J(z) = \sum_{i=0}^{JL} \beta_i z^{-i}$ on the entire complex plane. Observing that $H^J(z)$ is formed by all the roots of $H(z)$ with multiplicity J, we can extract from the roots of $H^J(z)$ those L roots that form $H(z)$. This implies that $H(z)$ is uniquely identifiable up to a scalar ambiguity.

Because $1 \leq J \leq Q$, choosing $R \geq QL+1$ distinct signature roots $\{\rho_r\}_{r=0}^{R-1}$ guarantees channel identifiability for any constellation of size Q, as we summarize in the following proposition:

Proposition 2: If the code period is selected to satisfy $R \geq QL+1$ and $\{\rho_r\}_{r=0}^{R-1}$ are distinct, identifiability of the Lth-order channel $H(z)$ is guaranteed from the received data $y(i;\, r) = H(\rho_r) s(i;\, r)$, for symbols $s(i;\, r)$ drawn from any constellation of size Q.

For a given constellation, however, it is possible to find $J \leq Q$, and alleviate the requirements on the period length R that guarantees channel identifiability (e.g., for QAM signals, $J = 4$ and $R \geq 4L + 1$ is enough).

B. Blind Channel Estimation Algorithms

Proposition 2 motivates the following general blind channel estimation algorithm in the presence of additive zero-mean, *complex circular* Gaussian noise (i.e., the real and imaginary parts of the noise are uncorrelated and Gaussian distributed).

Step 1) For zero-mean complex circular Gaussian noise $\tilde{\eta}(i; r)$, we have $E\{\tilde{\eta}^j(i; r)\} = 0, \forall\, j \in [1, J]$; hence, for the J defined after (17), it holds that

$$E\left\{y^J(i; r)\right\} = E\left\{[H(\rho_r)s(i; r) + \tilde{\eta}(i; r)]^J\right\} = H^J(\rho_r)E\left\{s^J(i; r)\right\}. \quad (19)$$

If $s(i; r)$ are equiprobable, then $E\{s^J(i; r)\} \neq 0$ (see Appendix II). Hence, we can find the Jth power of the channel from (19) as: $H^J(\rho_r) = E\{y^J(i; r)\}/E\{s^J(i; r)\}$. In practice, $E\{y^J(i; r)\}$ is replaced by consistent sample averages and thus, for each $r \in [0, R-1]$, $H^J(\rho_r)$ is estimated as:

$$\hat{H}^J(\rho_r) = \frac{1}{E\{s^J(i; r)\}} \left(\frac{1}{I}\sum_{i=0}^{I-1} y^J(i; r)\right) \quad (20)$$

where I is the total number of symbol blocks collected.

Step 2) Using $\{\hat{H}^J(\rho_r)\}_{r=0}^{R-1}$ obtained from Step 1, define $\hat{\tilde{\mathbf{h}}}_J := [\hat{H}^J(\rho_0), \ldots, \hat{H}^J(\rho_{R-1})]^T$, $\boldsymbol{\beta} := [\beta_0, \ldots, \beta_{JL}]^T$ and matrix $\mathbf{V}_J := [\mathbf{v}(\rho_0, JL+1), \ldots, \mathbf{v}(\rho_{R-1}, JL+1)]^T$, where $\mathbf{v}(\rho, D) := [1, \rho^{-1}, \ldots, \rho^{-D+1}]^T$ is a $D \times 1$ Vandermonde vector formed by the constant ρ. Observing that $\hat{\tilde{\mathbf{h}}}_J = \mathbf{V}_J\boldsymbol{\beta}$, it follows that $\boldsymbol{\beta}$ can be estimated as: $\hat{\boldsymbol{\beta}} = \mathbf{V}_J^{\dagger}\hat{\tilde{\mathbf{h}}}_J$, where $\dagger$ denotes matrix pseudoinverse.

Step 3) To obtain $\hat{\mathbf{h}}$ from $\hat{\boldsymbol{\beta}}$, we pursue a root-selection (RS) algorithm as follows.

S3.1) Generate the polynomial $p(x) = \hat{\beta}_0 + \hat{\beta}_1 x + \cdots + \hat{\beta}_{JL}x^{JL}$, and find its JL roots;

S3.2) Choose L out of the JL roots in S3.1, and using these L roots form polynomials $\gamma_0 + \gamma_1 x + \cdots + \gamma_L x^L$. With $C_{JL}^L := (JL)!/[L!(JL-L)!]$ denoting the number of possible L-root combinations, and $\boldsymbol{\gamma} := [\gamma_0 \cdots \gamma_L]^T$, we estimate the channel vector as

$$\hat{\mathbf{h}} = \arg\min_{\boldsymbol{\gamma}} \|\hat{\boldsymbol{\beta}} - \boldsymbol{\gamma} \star_J \boldsymbol{\gamma}\|. \quad (21)$$

Reminiscent of nonlinear synchronization circuits (e.g., squaring loops), we have shown how raising the received data $y(i; r)$ in (16) to the appropriate power enables (even blind) channel estimation in GFH-OFDMA transmissions.

From a complexity perspective, Step 1 is computationally simple; Step 2 involves matrix inversion, but since $\mathbf{V}_J$ is a constant matrix for each user, its inverse can be precomputed; Step 3 has complexity proportional to C_{JL}^L, so when J, L are moderate (say $\leq$4), complexity is reasonable. However, complexity increases fast as J, L increase.

Apart from complexity, the RS algorithm will exhibit sensitivity when roots are to be found in the presence of noise. Keeping in mind complexity and noise insensitivity issues, we developed several alternatives for Step 3 that we describe next.

A1) Minimum Distance (MD) Approach: For each $r \in [0, R-1]$, we have $H(\rho_r) = \lambda_r[H^J(\rho_r)]^{1/J}$, where $\lambda_r \in \{\exp(j2\pi n/J)\}_{n=0}^{J-1}$ is the corresponding scalar ambiguity in taking the Jth root. To resolve these ambiguities, we define $\tilde{\mathbf{h}}_1 := [\lambda_0[H^J(\rho_0)]^{1/J}, \ldots, \lambda_{R-1}[H^J(\rho_{R-1})]^{1/J}]^T$ and the matrix $\mathbf{V}_1 := [\mathbf{v}(\rho_0, L+1), \ldots, \mathbf{v}(\rho_{R-1,L+1})]^T$. There are J^R possible $\tilde{\mathbf{h}}_1$ vectors and for each one of them, we compute $\mathbf{h}_1 = \mathbf{V}_1^{\dagger}\tilde{\mathbf{h}}_1$. Our channel estimate can then be found based on a minimum Euclidean distance criterion as

$$\hat{\mathbf{h}} = \arg\min_{\mathbf{h}_1} \|\hat{\boldsymbol{\beta}} - \mathbf{h}_1 \star_J \mathbf{h}_1\|. \quad (22)$$

Recalling that a maximum-likelihood approach for joint channel and symbol estimation would require testing N symbols (usually $N \gg L$) over all possible choices from the finite alphabet of size Q, this MD approach reduces complexity from Q^N to J^R ($Q \geq J$). Although the MD approach is still too complex to be implemented in practice when $R \gg 1$, it is useful as a bound to benchmark performance of simpler channel estimates.

A2) Root Optimization (RO) Approach: Instead of picking L out of the JL noisy roots of $H^J(z)$ as in RS, we can optimize our selection. Specifically, minimizing the cost function $\mathcal{E} = \sum_{r=0}^{R-1} |H^J(\rho_r) - [\zeta_0 \prod_{i=1}^{L}(1 - \zeta_i\rho_i^{-1})]^J|^2$ over $\{\zeta_i\}_{i=0}^{L}$, we can form the channel transfer function as: $H(z) = \zeta_0 \prod_{i=1}^{L}(1 - \zeta_i z^{-1})$. Requiring nonlinear search, this method faces convergence and local minima problems. However, if one starts with root estimates obtained from the RS method, our experience with simulations is that the RO iteration converges fast to the global minimum and alleviates noise sensitivity problems associated with the RS algorithm.

A3) Linear Equations (LE)-Based Approach: Let us start from the simplest modulation (BPSK, $J = 2$) and define $\boldsymbol{\beta}_2 := [\beta_0, \ldots, \beta_{2L}]^T$, where $\beta_l = \sum_{i=0}^{l} h(i)h(l-i)$, $l = 0, 1, \ldots, 2L$. Here, we estimate $h(l)$ from β_l using the following forward elimination (backward substitution). Within a sign ambiguity (inherent to all blind channel estimators), we obtain $h(0)$ first as $h(0) = \sqrt{\beta_0}$; then, we recover sequentially $h(1), \ldots, h(L)$, using $h(l) = [\beta_l - \sum_{i=0}^{l-1} h(i)h(l-1-i)]/[2h(0)]$. When $|h(L)| \gg |h(0)|$, it is better to apply sequential recovery backward starting with $h(L) = \sqrt{\beta_{2L}}$. We then proceed to recover $h(L-1), \ldots, h(0)$ using $h(l) = [\beta_{l+L} - \sum_{i=l+1}^{L} h(i)h(l+L-i)]/[2h(L)]$.

It is straightforward to extend the LE-based channel estimator to a general $J > 2$. When J is power of 2, we can just apply the LE approach for $J = 2$ repeatedly.

Although simple to implement, the LE method is sensitive to noise when $h(0)$ or $h(L)$, is small. However, when we can guarantee that $|\hat{\beta}_0|$ or $|\hat{\beta}_{JL}|$ is strong enough (e.g., when the strongest path is synchronized to be the first path), then we can

apply the LE method in the forward or backward direction to obtain reliable channel estimates.

To further improve channel recovery, we can exploit the finite alphabet property (see also [15]) of $s(i;\, r)$ to robustify channel estimates obtained via RS or LE methods using the following decision-directed (DD) steps.

1) Set $i_1 = 1$, and find an initial estimate $\hat{\mathbf{h}}^{(1)}$ using the RS or the LE method. For every symbol index $k = iR + r$, with $i \in [0,\, I-1]$ and $r \in [0,\, R-1]$, detect the data as: $\tilde{s}^{(1)}(k) = \mathbf{v}^T(\rho_k,\, L+1)\hat{\mathbf{h}}^{(1)}y(k)$ and project $\tilde{s}^{(1)}(k)$ onto the finite alphabet to obtain the discrete values $\hat{s}^{(1)}(k)$.
2) In each successive iteration, $i_1 := i_1 + 1$.
   a) Define the vector $\mathbf{y} := [y(0), \ldots, y(IR-1)]^T$, the diagonal matrix $\hat{\mathbf{S}}^{(i_1-1)} := \mathrm{diag}\,(\hat{s}^{(i_1-1)}(0)\cdots\hat{s}^{(i_1-1)}(IR-1))$, and the $(L+1)\times IR$ Vandermonde matrix $\mathbf{G} := [\mathbf{v}(\rho_0,\, L+1), \ldots, \mathbf{v}(\rho_{IR-1},\, L+1)]^T$; solve the least squares problem $\min_{\mathbf{h}} \|\mathbf{y} - \hat{\mathbf{S}}^{(i_1-1)}\mathbf{G}\mathbf{h}\|$, and find the i_1th channel estimate as $\hat{\mathbf{h}}^{(i_1)} = (\hat{\mathbf{S}}^{(i_1-1)}\mathbf{G})^{\dagger} = \mathbf{G}^{\dagger}(\hat{\mathbf{S}}^{(i_1-1)})^{-1}$.
   b) Recompute soft symbol estimates using the channel estimates from a) as : $\tilde{s}^{(i_1)}(k) = \mathbf{v}^T(\rho_k)\hat{\mathbf{h}}^{(i_1)}y(k)$, and project again onto the finite alphabet to obtain hard decisions $\hat{s}^{(i_1)}(k)$.
3) Repeat step 2 several times (say I_1 times), or, continue until $\hat{\mathbf{S}}^{(i_1)} \approx \hat{\mathbf{S}}^{(i_1-1)}$ in the Euclidean norm sense.

Because forming $\mathbf{G}^{\dagger}$ requires inversion of a constant $(L+1)\times(L+1)$ matrix and $\hat{\mathbf{S}}^{(i)}$ is diagonal, this DD algorithm is also computationally efficient. The main concern here is whether this DD iteration converges. Given good initial channel estimates obtained with the RS or the LE method, our simulations confirmed that convergence occurs fast. A couple of remarks are now in order:

Remark 1: We need I to be sufficiently large so that the sample average in (20) converges to its ensemble counterpart. This in turn allows only sufficiently slow channel variations over the I blocks needed for estimation so that the channel can be considered time-invariant during this period (note that this assumption is common to the existing alternatives [6], [15], [18], [19]). However, we observe that $s^J(i;\, r)$ usually takes less values, e.g., three distinct values for 16 QAM signaling, which relaxes the requirement on I. Furthermore, for PSK constellations $\{\exp(j2\pi q/Q + j\pi/Q)\}_{q=0}^{Q-1}$ we do not even require sample averaging because $s^Q(i;\, r) = -1$ deterministically. Therefore, for PSK transmissions our channel estimators do not rely on statistical properties of $s(i;\, r)$ and it is thus not necessary to collect many blocks. At high signal-to-noise ratio (SNR), I can be as small as 1, which relaxes the requirement for channel invariance and reduces decoding delay. When I is set to be 1 at high SNR, BPSK (QPSK) signals with $Q = 2$ ($Q = 4$) require that the channel remains invariant for only $R \geq 2L+1$ ($R \geq 4L+1$) blocks. In contrast, note that [6], [18], and [19] depend on the correlation matrix of the received data block, and one needs to collect many blocks to approximate the true correlation matrix with its sample estimate.

Remark 2: Although we have dealt in this paper with multiuser transmissions, our blind channel estimators can be applied directly to single-user OFDM [1]. So long as one transmits over $R \geq QL+1$ subcarriers, channel identifiability is guaranteed based on a single received data block, which is not the case for the subspace-based method in [7], where the channel is not allowed to have nulls located on subcarriers. Relative to the subspace method of [13] that relies on zero-padded IBI-free transmitted blocks to guarantee channel identifiability, our channel estimators herein are capable of identifying FIR channels even from a single received block when PSK modulations are employed. Furthermore, for moderate J and L, our method is computationally more efficient than the subspace-based methods of [7] and [13] that require singular value decomposition of matrices with dimensionalities $(2P-L)\times(2P-2L)$ and $P\times P$, respectively.

V. Slow- and Fast-Hopping of Signature Points

The signature points $\{\rho_{m,k}\}_{m=1}^{M}$ we selected to design our MUI-elimination codes in Section III were allowed to vary from symbol to symbol. Depending on their rate of variation, we will focus in this section on slow- and fast-hopping systems.

A. Slow-Hopping

Consider a slow-hopping system with W symbols per hop that relies on R distinct signature points per user. The period of the long code is then WRP and, spread over the code of each user's signature point, W symbols are transmitted per hop. We will express the symbol index as: $k = i(WR) + rW + w$, $r \in [0,\, R-1]$, $w \in [0,\, W-1]$, and we will denote as $(i;\, r;\, w)$ the argument $(iWR+rW+w)$, where i is the index of a WR-long block of symbols, r is the index of distinct signature points within the symbol block, and w is the symbol index inside each hop. Proposition 2 still holds true, and Step 1 for channel estimation changes accordingly to

$$\hat{H}_m^J(\rho_{m,r}) = \frac{1}{E\{s_m^J(i;\, r;\, w)\}}\,\frac{1}{WI}\sum_{i=0}^{I-1}\sum_{w=0}^{W-1} y_m^J(i;\, r;\, w). \tag{23}$$

Note that now we need at least WR symbol blocks (with $I = 1$) in (23) and thus require slower channel variations. Steps 2 and 3 in our channel estimation algorithms remain the same, and once CSI is acquired at the receiver, the transmitted symbols are recovered using

$$\hat{s}_m(i;\, r;\, w) = y_m(i;\, r;\, w)/\hat{H}_m(\rho_{m,r}) \tag{24}$$

where $\hat{H}_m(\rho_{m,r})$ denotes the channel estimated using any of the methods in Section IV.

B. Fast-Hopping

Thanks to signature point hopping, users in our GFH-OFDMA system will not suffer from severe fading persistently because no single transmission will be hit consistently by channel nulls. In addition, changing bursty errors to distributed errors, one expects system performance to

improve considerably through channel coding. To illustrate the advantage of GFH-OFDMA over conventional coded OFDMA, we specify here the channel code to be the simplest repetition code; namely, we adopt symbol transmission via several signature points (or frequencies), which corresponds to nothing but a fast-hopping system. Suppose that we use an $(1, T)$ repetition code and let R be a multiple of T, say $R = WT$, which means that there are W symbols transmitted during one long code period RP. For clarity, we express $r = wT + t$, $r \in [0, R-1]$, $w \in [0, W-1]$, $t \in [0, T-1]$ and denote $x(i; r) := x(i; w; t)$. Proposition 2 still holds true and the blind channel identification methods of Section IV are directly applicable. They will yield reliable estimates when I is large enough so that the sample average in (20) converges to its ensemble counterpart (recall that for PSK transmissions, $I = 1$ is sufficient at high SNR). Once the channels have been estimated, symbols can be recovered using a maximum-ratio combining (matched filter) decoder as

$$\begin{aligned}\hat{s}_m(i; w) &= \sum_{t=0}^{T-1} \hat{H}_m^*(\rho_{m,w,t}) y_m(i; w; t) \\ &= \sum_{t=0}^{T-1} \left|\hat{H}_m(\rho_{m,w,t})\right|^2 s_m(i; w) \\ &\quad + \sum_{t=0}^{T-1} \hat{H}_m^*(\rho_{m,w,t}) \eta_m(i; w; t). \end{aligned} \tag{25}$$

Note that channels of maximum order L have at most L roots, and if we choose $T \geq L+1$, symbol recovery is always guaranteed, which is never the case for conventional OFDMA, no matter how large T is chosen. Although bandwidth is expanded when $T \geq L+1$, improved performance may justify such an expansion in, e.g., military applications. Even though symbol recovery is not guaranteed with $1 < T \leq L$, symbol-error rate performance improves significantly with fast hopping because the larger T is, the less likely it becomes to have at the same time all T signature points coincide with channel nulls.

VI. Performance Analysis and Simulations

In our MUI-free GFH-OFDMA received data in (12), the multipath channel $\mathbf{h}_m$ affects the mth user's performance through the flat fading factor $\mathbf{g}_m^T(k)\mathbf{C}_m(k)\mathbf{h}_m = H_m(\rho_{m,k})$. We have R distinct signature points $\{\rho_{m,r}\}_{r=0}^{R-1}$ per user, and by letting $k = iR + r$, we have $\mathbf{g}_m(k) = \mathbf{g}_m(r)$, $\forall\, i$. Because for each $r \in [0, R-1]$, we have

$$\mathbf{g}_m^T(r)\mathbf{x}(i; r) = H_m(\rho_{m,r}) s_m(i; r) + \mathbf{g}_m^T(r)\boldsymbol{\eta}(i; r). \tag{26}$$

If $E\{|s_m(i; r)|^2\} = \sigma_{s,m}^2$ and the additive noise $\eta(t)$ has two-sided power density $N_0/2$, then our Signal to Noise Ratio (SNR) will be $|H_m(\rho_{m,r})|^2 \sigma_{s,m}^2 / (N_0 \|\mathbf{g}_m(r)\|^2/2)$. With $2E_s/N_0$ denoting symbol SNR, we have $\sigma_{s,m}^2 = E_s/E_{cm,r}$, where $E_{cm,r} := \sum_{n=0}^{P-1} |c_m(r; n)|^2$ is the energy of the mth user's code when $\rho_{m,r}$ is used; hence

$$\text{SNR}_m(r) = |H_m(\rho_{m,r})|^2 \, \frac{1}{\|\mathbf{g}_m(r)\|^2 E_{cm,r}} \, \frac{2E_s}{N_0}. \tag{27}$$

For simplicity, we will adopt BPSK signaling with bit SNR $2E_b/N_0 = 2E_s/N_0$. Therefore, our system's bit-error rate (BER) can be found in closed form as [9, p. 773]: $P_{e,m}(r) = \mathcal{Q}(\sqrt{SNR_m(r)})$, where $\mathcal{Q}(\cdot)$ denotes the $\mathcal{Q}$-function.

Recalling that we have R distinct signature points $\rho_{m,r}$, the performance of the mth user will be the average BER averaged over all R roots: $P_{e,m} = (1/R)\sum_{r=0}^{R-1} P_{e,m}(r)$. From (27), the average BER $P_{e,m}$ can be expanded as

$$\begin{aligned} P_{e,m} &= \frac{1}{R} \sum_{r=0}^{R-1} P_{e,m}(r) \\ &= \frac{1}{R} \sum_{r=0}^{R-1} \mathcal{Q}\left(|H_m(\rho_{m,r})| \sqrt{\frac{1}{\|\mathbf{g}_m(r)\|^2 E_{cm,r}}} \sqrt{\frac{2E_b}{N_0}} \right). \end{aligned} \tag{28}$$

For codes chosen as in (15), the BER in (28) reduces to

$$P_{e,m} = \frac{1}{R} \sum_{r=0}^{R-1} \mathcal{Q}\left(\left| H_m\left(e^{j((2\pi/M)m + \theta_r)}\right)\right| \sqrt{\frac{2E_b}{N_0}} \right). \tag{29}$$

In comparison, the BER for an M-user OFDMA system at the mth receiver's output is

$$P_{e,m} = \mathcal{Q}\left(\left| H_m\left(e^{j(2\pi m/M)}\right)\right| \sqrt{\frac{2E_b}{N_0}} \right) \tag{30}$$

which is obtained from (29) by setting $R = 1$ and $\theta_r = 0$.

In addition to our closed BER forms, we also tested performance of our GFH-OFDMA system with extensive simulations, a sample of which we describe next.

Test Case 1 (The Advantage of FH in OFDMA): We compare (29) that corresponds to FH-OFDMA with (30) that corresponds to OFDMA on an $M = 16$ user system transmitting through Rayleigh fading multipath channels of order $L = 2$ (three rays). For FH-OFDMA, we select $R = 16$, and perform 500 Monte Carlo realizations. Although for a specific channel realization the BER averaged over all users may be significantly lower in FH-OFDMA relative to that in conventional OFDMA, the improvement disappears when we also average over all possible channel realizations, as shown in Fig. 3(a). However, the advantage of FH-OFDMA over standard OFDMA can be appreciated when evaluating how far the real performance would be from its average, which measures reliability of the transmission link. Fig. 3(b) shows that FH-OFDMA exhibits much lower standard deviation compared to conventional OFDMA, which demonstrates the advantage of FH.

Test Case 2 (The Advantage of MUI-Free Reception): To illustrate the advantage of structured GFH-OFDMA over long PN code DS-CDMA with RAKE reception, we simulate GFH-OFDMA with $R = M = 16$ signature points $\{\rho_{k,m} = [1 + 0.1\cos(\pi \overline{k}_m/2)]\exp(j2\pi \overline{k}_m/M)\}$, where $\overline{k}_m = (k+m) \bmod M$. Without hopping ($\overline{k}_m = m$), these codes were also used in [12] to show resilience to Doppler effects. We also implement two long code DS-CDMA systems with code lengths $P = 16$ over 100 Rayleigh fading channels of order $L = 2$. The first DS-CDMA system adopts symbol periodic OFDM codes $\tilde{c}_m(n) = \exp(j2\pi mn/M)$ scrambled by $\overline{c}(k; n) = \exp(j\phi_{k,n})$, where $\phi_{k,n}$ is uniformly distributed in

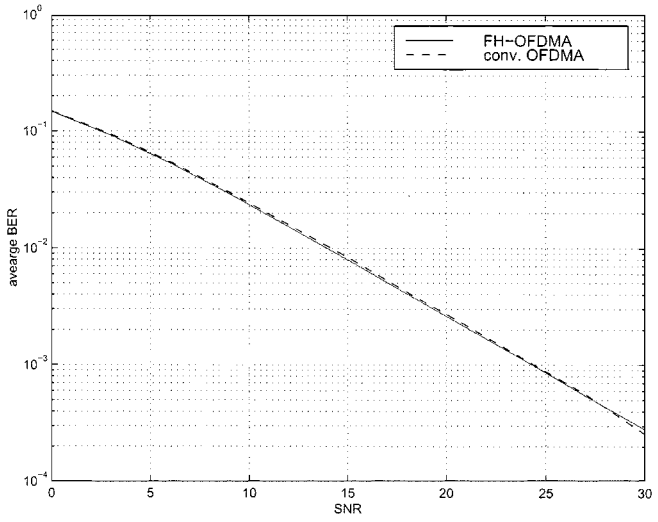

(a)

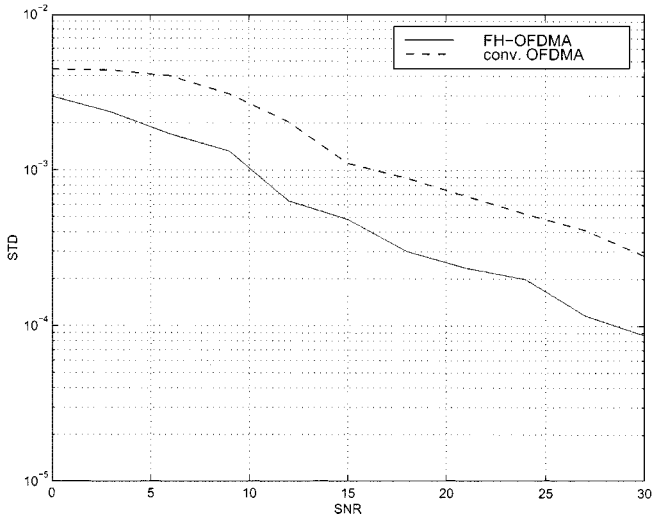

(b)

Fig. 3. Comparisons of FH-OFDMA with conventional OFDMA. (a) Mean BER. (b) STD BER.

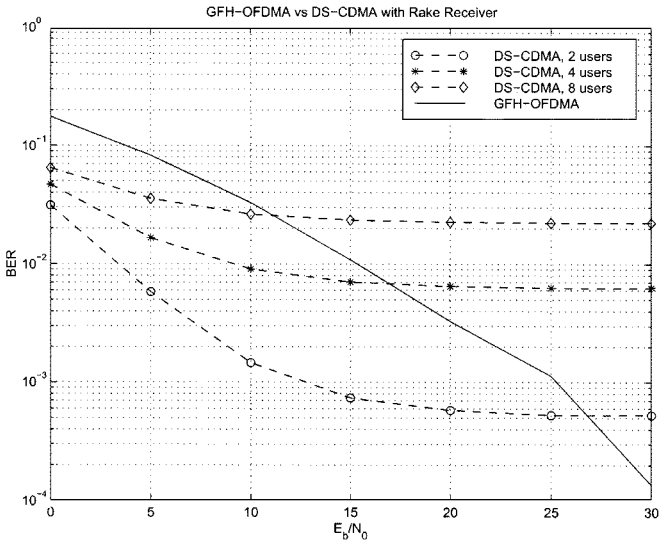

(a)

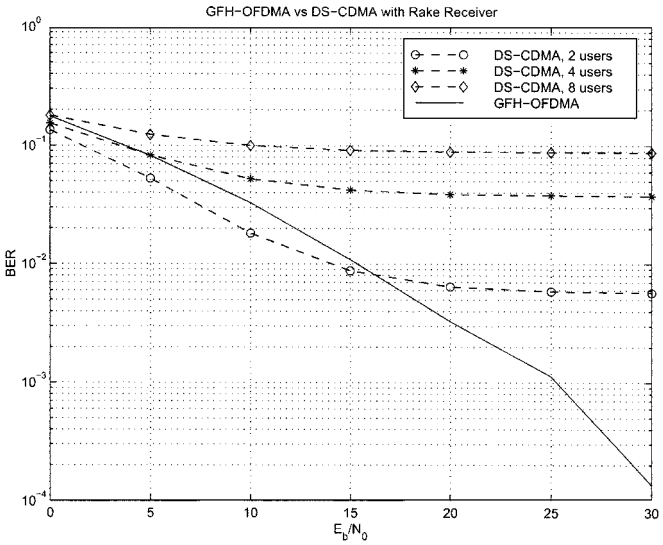

(b)

Fig. 4. Comparisons of GFH-OFDMA with long code DS-CDMA. (a) OFDM codes. (b) W-H codes.

$[0, 2\pi]$; while the second utilizes IS-95 like Walsh–Hadamard codes scrambled by random $\{\pm 1\}$ sequences. Fig. 4(a) and (b) confirms that OFDM codes perform better against multipath than W–H codes, which is expected because OFDM codes have smaller cross correlations with their delayed versions than W–H. However, both suffer from MUI severely when the system load increases (e.g., when $M = 8$ which corresponds to 50% load). MUI-free GFH-OFDMA clearly outperforms long-code DS-CDMA under moderate system load and SNR, as confirmed by the average BER curves depicted in Fig. 4(a) and (b).

Test Case 3 (Blind Channel Estimation and Equalization): To check the algorithms outlined in Section IV, we adopt the code design (15), set $R = M = 16$, $L = 2$, and simulate them over 500 randomly generated channels. Figures of merit here are the normalized least-squares channel error (NLSE): $||\mathbf{h}_m - \hat{\mathbf{h}}_m||^2/||\mathbf{h}_m||^2$, and the BER evaluated based on the obtained channel estimates. For BPSK signaling ($J = 2$), we adopt $I = 30$; thus, $N = IR = 480$ symbols are used for channel estimation. Fig. 5(a) and (b) depicts channel NLSE and BER, respectively, using the minimum distance (MD), the RS, the RS followed by one step ($I_1 = 1$) DD iteration (RS-DD), and the RS followed by root optimization (RS-RO). Fig. 5(b) shows that BERs relying on estimated channels are close to the ideal scenario where perfect CSI is available. To apply these channel estimators to QPSK signaling ($J = 4$), we use $I = 50$, and thus $N = IR = 800$ symbols to average out noisy cross-terms [note that $y_m^4(i; r)$ introduces additional noisy terms relative to BPSK]. Fig. 6(a) and (b) shows NLSE and BER, respectively, for QPSK signaling, while here $I_1 = 5$ iterations are performed for the RS-DD channel estimator. We observe that RS performs worse when J increases, because L roots must be chosen out of a bigger set of JL noisy roots, and matching those L roots with multiplicity J with the original JL roots in the frequency domain becomes less reliable. However, when followed up by sufficient DD steps, its performance comes close to the ideal case. On the other hand, we observe that MD and RS-RO

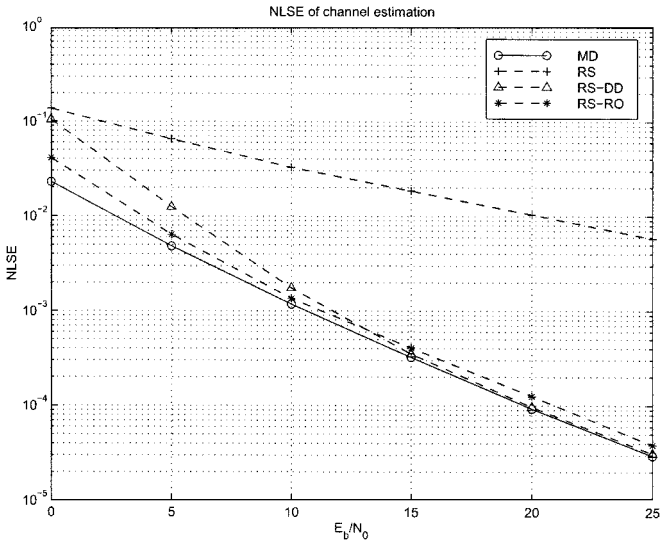

(a)

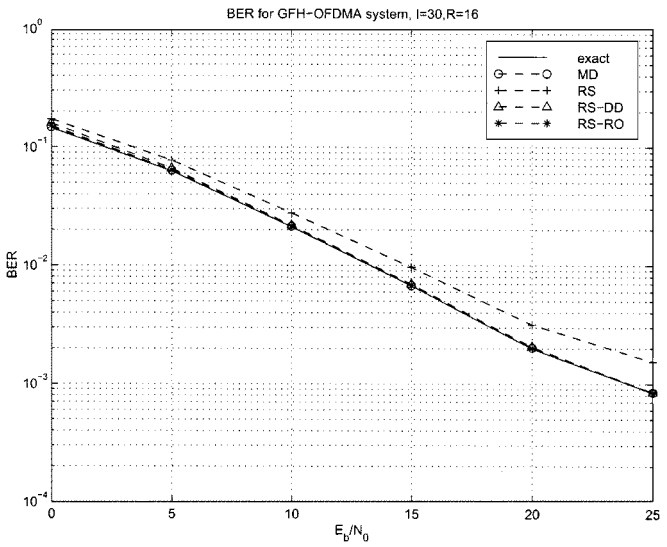

(b)

Fig. 5. Blind channel estimation (BPSK). (a) Channel NLSE. (b) BER.

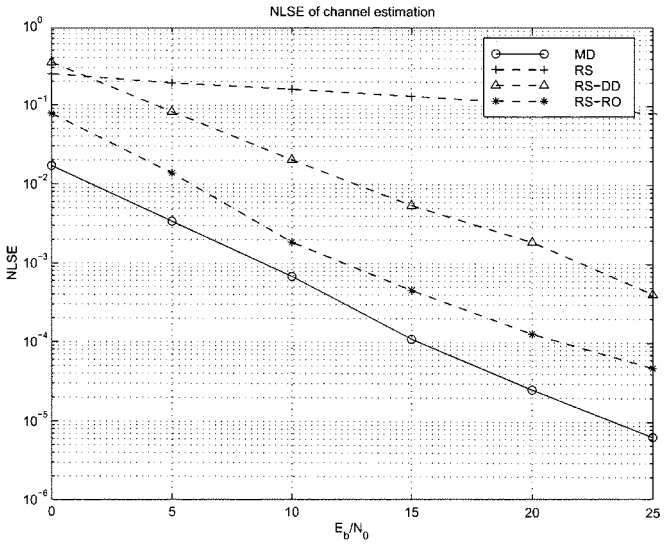

(a)

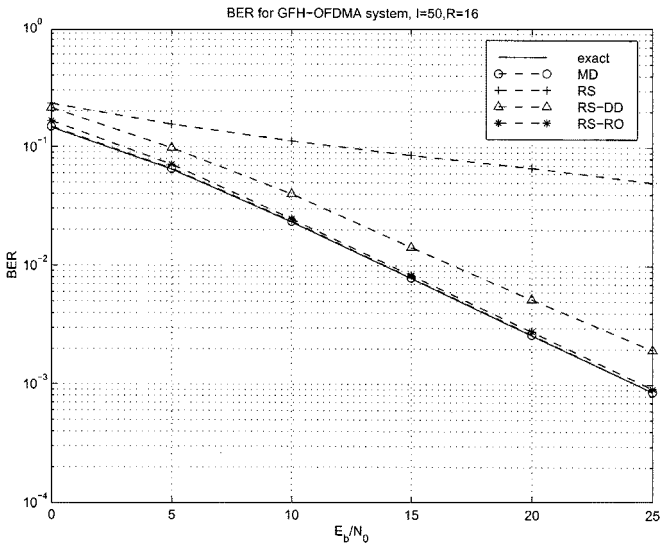

(b)

Fig. 6. Blind channel estimation (QPSK). (a) Channel NLSE. (b) BER.

are robust to noise and variable signal constellation sizes as expected.

Performance of the LE estimator is channel-dependent. Specifically, if the first path is guaranteed to be strong enough for the user of interest, the LE algorithm yields reliable channel estimates. For QS multiuser systems not all users' direct paths will be always strong enough due to relative delays; thus, we recommend applying the LE channel estimators only to those users that have strong first (or last) path. To test the LE estimator, we use the code design in (15), set $R = M = 16$, $L = 2$, and simulate 500 random channels having their first path to be the strongest one. Due to space limitations, we only plot the overall system BER with estimated channels. Fig. 7(a) uses $I = 30$ blocks to compute BER of BPSK signals using the RS, the RS followed by one DD step, the LE, and the LE followed by one DD iteration. Fig. 7(b) is the counterpart of Fig. 7(a) but for QPSK signals with $I = 50$ and five DD iterations following the RS and two DD iterations following the LE channel estimator. We see clearly that the LE outperforms the RS estimator and is capable of approaching the ideal performance in very few iterations, while being extremely simple to implement.

Test Case 4 (Application to OFDM Systems): Our blind channel estimation is directly applicable to single-user OFDM. To compare the LE estimator with subspace alternatives of comparable equalization complexity, we use $R = 32$ subcarriers and the measured channel $\mathbf{h} = [0.66, -0.46, -0.28, -0.22, 0.12]$ as in [7]. With BPSK signaling and similar to [7], we overestimated the channel order as $L = 8$. Because for QPSK signaling we need $R \geq 4L+1$ for the LE estimator, we adopted $L = 4$ for both methods to assure a fair comparison. Fig. 8(a) shows the NLSE for both methods using 300 OFDM symbols averaged over 500 Monte-Carlo runs. Subspace-based methods are constellation-independent and with the same bit energy E_b, QPSK signals have twice the symbol energy of a BPSK symbol; thus, channel estimation accuracy improves. However, the LE channel estimator is constellation-dependent and as shown in Fig. 8(a), channel estimates for BPSK signaling are

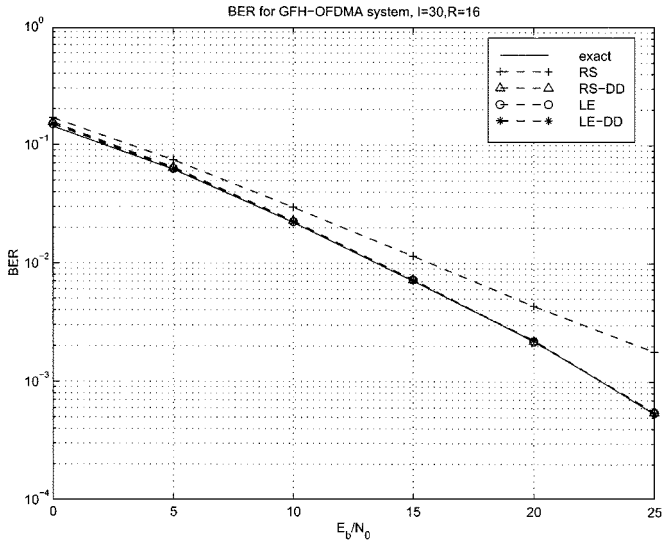

(a)

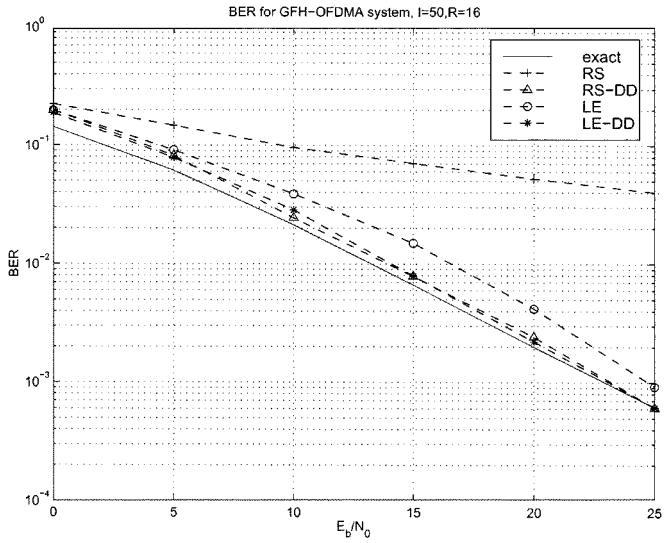

(b)

Fig. 7. Application of the LE method. (a) BPSK. (b) QPSK.

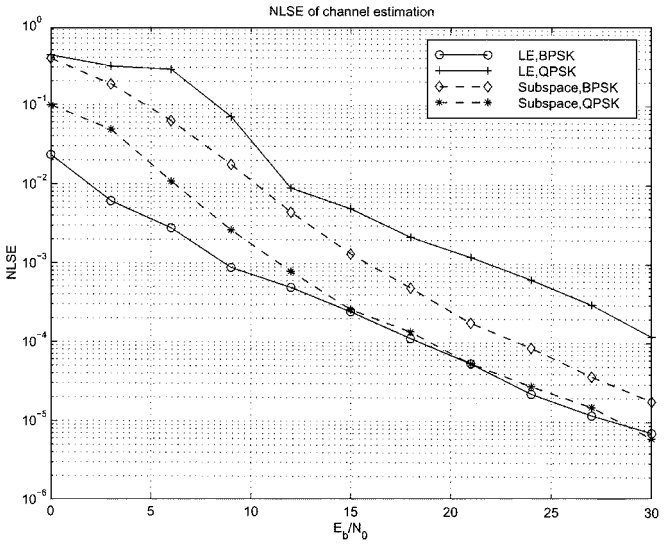

(a)

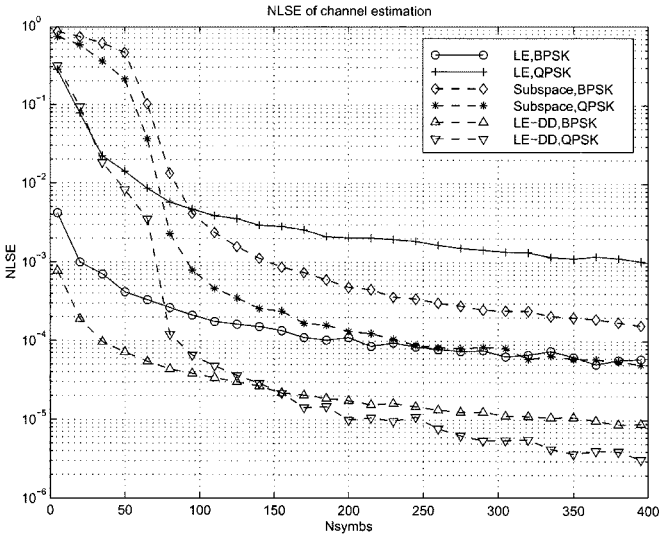

(b)

Fig. 8. Comparisons of the LE method with [7] in a single-user OFDM system. (a) NLSE versus E_b/N_0. (b) NLSE versus number of symbol blocks.

far better than those obtained for QPSK. Fig. 8(b) shows the relation between NLSE and the number of symbols used for channel estimation with $E_b/N_0 = 20$ dB. At least $2R = 64$ OFDM symbols should be collected for the subspace-based method to guarantee that the data covariance matrix is full rank, while even one symbol may be enough for the LE estimator at high SNR. We observe clearly that the LE channel estimator converges much faster. When only few symbols are available, we can apply the LE first and then improve accuracy with several DD iterations. With $I_1 = 1$ iterations, Fig. 8(b) shows that the NLSE using the LE-DD estimator is noticeably improved for both BPSK and QPSK signaling. Finally, we should reiterate that the LE guarantees channel identifiability from a single OFDM symbol while the subspace method will fail for channels with subcarrier nulls [7].

Test Case 5 (Fast Hopping): To check how much fast hopping improves our GFH-OFDMA system over conventional OFDMA, we adopt again the code design in (15), $M = R = 16$, $L = 2$ and simulate 500 random channels. Fig. 9 illustrates that the average performance is much better for GFH-OFDMA than for the conventional OFDMA when $T = 2$, even though symbol recovery is not guaranteed for GFH-OFDMA in this case. Note that whatever T is, symbol recovery is not guaranteed for conventional OFDMA, while by setting $T = 4 \geq L + 1$, symbol recovery is assured for GFH-OFDMA, which explains why the gap between these two systems increases as evidenced in Fig. 9.

VII. Conclusions and Discussion

We developed in this paper a general CDMA system utilizing structured symbol-aperiodic long codes, which bridges long code DS-CDMA with frequency-hopped multicarrier transmissions. Superior to DS-CDMA with long PN codes and RAKE reception, GFH-OFDMA achieves MUI elimination deterministically by design, and relative to conventional OFDMA, it exhibits improved performance because no user

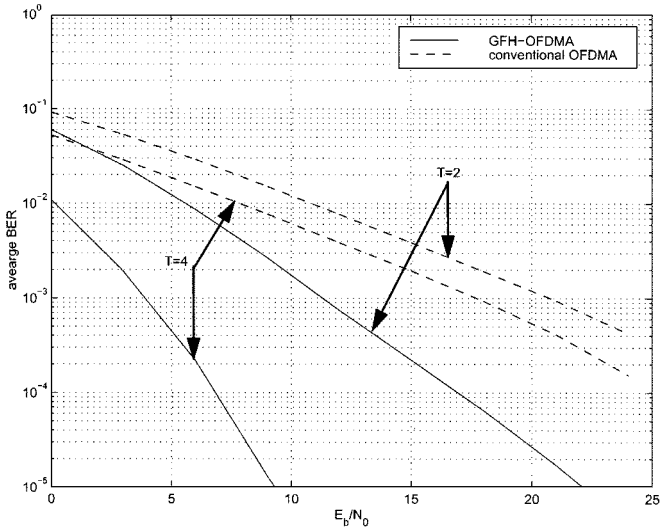

Fig. 9. Fast frequency-hopping.

suffers persistently from channel nulls. GFH-OFDMA outperforms conventional OFDMA when the same amount of redundancy is added in the form of fast hopping. We currently investigate an alternative GFH-OFDMA approach that relies on block-spreading to guarantee symbol recovery and resilience to interference [21].

Novel blind channel estimation methods were also derived in this paper based on the MUI-free received data and shown to guarantee channel identifiability for any finite signal constellation. In addition to the flexibility of trading off complexity with performance, the resulting channel estimators are also directly applicable to single-user OFDM over mobile channels [20], [].

Appendix I
Ddetermination of $H^J(\rho_r)$

Multiplying (17) by $H^Q(\rho_r)$ and substituting $H(\rho_r) = y(i;r)/s(i;r)$, we obtain

$$y^Q(i;r)+\alpha_1 y^{Q-1}(i;r)H(\rho_r)+\cdots+\alpha_Q H^Q(\rho_r)=0. \quad (31)$$

For each r, $y(i;r) = H(\rho_r)s(i;r)$ takes on at most Q distinct values as $s(i;r)$ is chosen from a finite alphabet set of size Q [we assume that $H(\rho_r) \neq 0$; otherwise, all outputs are zero and we obtain $H^J(\rho_r) = 0$]. Suppose we collect sufficient $y(i;r)$ samples so that for each ρ_r we have Q distinct samples $y(i_0;r), \ldots, y(i_{Q-1};r)$, where $i_0, \ldots, i_{Q-1}$ are the corresponding symbol block indices. By constructing the Vandermonde matrix

$$\tilde{\mathbf{Y}} := \begin{pmatrix} y^{Q-1}(i_0;r) & \cdots & y(i_0;r) & 1 \\ \vdots & \ddots & \vdots & \vdots \\ y^{Q-1}(i_{Q-1};r) & \cdots & y(i_{Q-1};r) & 1 \end{pmatrix} \quad (32)$$

and using (31), we arrive at

$$-\begin{pmatrix} y^Q(i_0;r) \\ \vdots \\ y^Q(i_{Q-1};r) \end{pmatrix} = \tilde{\mathbf{Y}} \begin{pmatrix} \alpha_1 & \cdots & 0 \\ \vdots & \ddots & \vdots \\ 0 & \cdots & \alpha_Q \end{pmatrix} \begin{pmatrix} H(\rho_r) \\ \vdots \\ H^Q(\rho_r) \end{pmatrix}. \quad (33)$$

Matrix $\tilde{\mathbf{Y}}$ is invertible for it is a Vandermonde matrix constructed from Q distinct points. Recalling that $\alpha_J \neq 0$, we can solve (33) to obtain $H^J(\rho_r)$, $\forall r \in [0, R-1]$.

Appendix II
Proof of $E\{s^J(k)\} \neq 0$

When data symbols are equiprobable, we have $E\{s^J(k)\} = (1/Q)\sum_{i=1}^{Q} \zeta_i^J$, where $\{\zeta_i\}_{i=1}^{Q}$ are signal points on complex plane. Therefore, we need to prove that $\sum_{i=1}^{Q} \zeta_i^J \neq 0$, when $\alpha_1, \ldots, \alpha_{J-1} = 0$, and $\alpha_J \neq 0$. Expansion of $\prod_{i=1}^{Q}(s(k)-\zeta_i)$ gives

$$\alpha_1 = -\sum_i \zeta_i, \qquad \alpha_2 = \sum_{i_1<i_2} \zeta_{i_1}\zeta_{i_2}, \ldots$$
$$\alpha_J = (-1)^J \sum_{i_1<\cdots<i_J} \zeta_{i_1}\ldots\zeta_{i_J} \quad (34)$$

where subscripts i, i_j, $\forall j$, are taken from the set $[1, Q]$.

Defining $\Theta_j = \sum_{i=1}^{Q} \zeta_i^j$, and applying Newton's identities ([8, p. 135]), we find

$$\Theta_J + \alpha_1\Theta_{J-1} + \cdots + \alpha_{J-1}\Theta_1 + J\alpha_J = 0. \quad (35)$$

Based on (35) and recalling that $\alpha_j = 0$, $\forall j \in [1, J-1]$, we obtain $E\{s^J(k)\} = (1/Q)\Theta_J = -(J/Q)\alpha_J \neq 0$. For PSK constellation of size Q: $\{\exp(j2\pi q/Q + j\pi/Q)\}_{q=0}^{Q-1}$, we can easily verify that $\alpha_j = 0$, $\forall j \in [1, Q-1]$, $\alpha_Q = 1$, and $(1/Q)\sum_i \zeta_i^Q = -\alpha_Q = -1$.

References

[1] J. A. C. Bingham, "Multicarrier modulation for data transmission: An idea whose time has come," *IEEE Commun. Mag.*, pp. 5–14, May 1990.

[2] Q. Chen, E. S. Sousa, and S. Pasupathy, "Multicarrier CDMA with adaptive frequency-hopping for mobile radio systems," *IEEE J. Select. Areas Commun.*, pp. 1852–1857, Dec. 1996.

[3] V. M. DaSilva and E. S. Sousa, "Multicarrier orthogonal CDMA signals for quasisynchronous communication systems," *IEEE J. Select. Areas Commun.*, pp. 842–852, June 1994.

[4] K. S. Gilhousen, I. M. Jacobs, R. Padovani, A. J. Viterbi, L. A. Weaver, and C. E. Wheatley III, "On the capacity of a cellular CDMA system," *IEEE Trans. Veh. Technol.*, vol. 40, pp. 303–312, May 1991.

[5] H. Liu, G. Xu, L. Tong, and T. Kailath, "Recent development in blind channel equalization: From cyclostationarity to subspace," *Signal Processing*, vol. 50, pp. 83–99, Apr. 1996.

[6] H. Liu and M. D. Zoltowski, "Blind equalization in antenna array CDMA systems," *IEEE Trans. Signal Processing*, vol. 45, pp. 161–171, Jan. 1997.

[7] B. Muquet, M. Courville, P. Duhamel, and V. Buzenac, "A subspace based blind and semi-blind channel identification method for OFDM systems," in *Proc. IEEE 2nd Workshop on Signal Processing Advances in Wireless Communications*, Annapolis, MD, May 9–12, 1999, pp. 170–173.

[8] J. Nathan, *Basic Algebra*. San Francisco, CA: Freeman, 1974.

[9] J. Proakis, *Digital Communications*, 3rd ed. New York: McGraw-Hill, 1995.

[10] H. Sari, "Orthogonal frequency-division multiple access with frequency-hopping and diversity," in *Multi-Carrier Spread Spectrum*, K. Fazel and G. P. Fettweis, Eds. Norwell, MA: Kluwer, 1997, pp. 57–68.

[11] H. Sari and G. Karam, "Orthogonal frequency-division multiple access and its application to CATV network," *Eur. Trans. Telecommun.*, vol. 9, no. 6, pp. 507–516, Nov./Dec. 1998.

[12] A. Scaglione and G. B. Giannakis, "Design of user codes in QS-CDMA systems for MUI elimination in unknown multipath," *IEEE Commun. Lett.*, vol. 3, pp. 25–27, Feb. 1999.

[13] A. Scaglione, G. B. Giannakis, and S. Barbarossa, "Redundant filterbank precoders and equalizers: Parts I and II," *IEEE Trans. Signal Processing*, vol. 47, pp. 1988–2022, July 1999.

[14] ——, "Lagrange/Vandermonde MUI eliminating user codes for quasisynchronous CDMA in unknown multipath," *IEEE Trans. Signal Processing*, vol. 48, pp. 2057–2073, July 2000.
[15] M. Torlak, B. L. Evans, and G. Xu, "Blind estimation of FIR channels in CDMA systems with aperiodic spreading sequences," in *Proc. 31st Asilomar Conf.*, Pacific Grove, CA, Nov. 2–5, 1997, pp. 495–499.
[16] M. K. Tsatsanis and G. B. Giannakis, "Optimal linear receivers for DS-CDMA systems: A signal processing approach," *IEEE Trans. Signal Processing*, vol. 44, pp. 3044–3055, Dec. 1996.
[17] Z. Wang, A. Scaglione, G. B. Giannakis, and S. Barbarossa, "Vandermonde–Lagrange mutually orthogonal flexible transceivers for blind CDMA in unknown multipath," in *Proc. IEEE 2nd Workshop on Signal Processing Advances in Wireless Communications*, Annapolis, MD, May 9–12, 1999, pp. 42–45.
[18] A. J. Weiss and B. Friedlander, "Channel estimation for DS-CDMA downlink with aperiodic spreading codes," *IEEE Trans. Commun.*, vol. 47, pp. 1561–1569, Oct. 1999.
[19] Z. Xu and M. K. Tsatsanis, "Blind channel estimation for long code multiuser CDMA systems," *IEEE Trans. Signal Processing*, vol. 48, pp. 988–1001, Apr. 2000.
[20] S. Zhou and G. B. Giannakis, "Finite-alphabet based channel estimation for OFDM and related multi-carrier systems," in *Proc. 34th Conf. Information Sciences and Systems (CISS'00)*, Princeton, NJ, Mar. 2000.
[21] S. Zhou, G. B. Giannakis, and A. Swami, "Frequency-hopped generalized MC-CDMA for multipath and interference suppression," in *Proc. MILCOM Conf.*, Los Angeles, CA, Oct. 2000, pp. 22–25.

Shengli Zhou (S'99) was born in Anhui, China, in 1974. He received the B.S. degree in 1995 and the M.Sc. degree in 1998, from the University of Science and Technology of China (USTC), all in electrical engineering and information science. He is now working toward the Ph.D. degree in the Department of Electrical and Computer Engineering at the University of Minnesota, Minneapolis.

His broad interests lie in the areas of statistical signal processing and communications, including transceiver optimization, blind channel estimation and equalization algorithms, multicarrier, space–time signal processing, spread-spectrum systems.

Georgios B. Giannakis (F'97) received the Diploma in electrical engineering from the National Technical University of Athens, Athens, Greece, in 1981. From September 1982 to July 1986, he was with the University of Southern California (USC), Los Angeles, where he received the MSc. degree in electrical engineering in 1983, the MSc. degree in mathematics in 1986, and the Ph.D. degree in electrical engineering in 1986.

After lecturing for one year at USC, he joined the University of Virginia, Charlottesville, in 1987, where he became a Professor of Electrical Engineering in 1997. Since 1999, he has been with the University of Minnesota, Minneapolis, as a Professor of Electrical and Computer Engineering. His general interests span the areas of communications and signal processing, estimation and detection theory, time-series analysis, and system identification—subjects on which he has published more than 120 journal papers, 250 conference papers, and two edited books. Current research topics focus on transmitter and receiver diversity techniques for single- and multiuser fading communication channels, redundant precoding and space–time coding for block transmissions, multicarrier, and wide-band wireless communication systems.

Dr. Giannakis has co-authored three papers that received Best Paper Awards from the IEEE Signal Processing (SP) Society (1992, 1998, 2000). He also received the Society's Technical Achievement Award in 2000. He co-organized three IEEE-SP Workshops (HOS in 1993, SSAP in 1996, and SPAWC in 1997) and guest (co-) edited four special issues. He has served as an Associate Editor for the IEEE TRANSACTIONS ON SIGNAL PROCESSING and the IEEE SIGNAL PROCESSING LETTERS. He is a secretary of the SP Conference Board, a member of the SP Publications Board and a member and Vice-Chair of the Statistical Signal and Array Processing Committee. He is a member of the Editorial Board for the PROCEEDINGS OF THE IEEE, he chairs the SP for Communications Technical Committee and serves as the Editor-in-Chief for the IEEE SIGNAL PROCESSING LETTERS. He is a member of the IEEE Fellows Election Committee, the IEEE-SP Society's Board of Governors, and a frequent consultant for the telecommunications industry.

Anna Scaglione (M'99) received the M.Sc. and Ph.D. degrees from the University of Rome "La Sapienza," Rome, Italy, in 1995 and 1999, respectively.

During 1997, she was at the University of Virginia, Charlottesville, as Visiting Research Assistant. In 1999 she was a Postdoctoral Researcher at the University of Minnesota, Minneapolis. She recently joined the University of New Mexico, Albuquerque, as an Assistant Professor. Her broad research area is signal processing for communications and her work has been focused on optimal design of modulation and multiplexing techniques for frequency-selective, time-varying channels.